PERGAMON

Solid State Communications 115 (2000) 329–333

solid state communications

www.elsevier.com/locate/ssc

Carrier–carrier scattering: an experimental comparison of 5 and 3 nm $Al_xGa_{1-x}As$/GaAs quantum wells

K.W. Sun[a,*], C.-K. Sun[b], J.C. Wang[b], S.Y. Wang[c], C.P. Lee[c]

[a]*Department of Electronic Engineering, Feng Chia University, Taichung 407, Taiwan, ROC*
[b]*Department of Electrical Engineering and Graduate Institute of Electro-Optical Engineering, National Taiwan University, Taipei, Taiwan, ROC*
[c]*Department of Electronics Engineering and Institute of Electronics, National Chiao Tung University, Hsin Chu, Taiwan, ROC*

Received 14 February 2000; received in revised form 21 March 2000; accepted 22 March 2000 by H. Akai

Abstract

We have studied carrier dynamics among highly nonequilibrium carrier distributions generated with femtosecond laser pulses in Be:$Al_xGa_{1-x}As$/GaAs quantum wells with different well width at hot carrier densities between 10^9 and 10^{11} cm^{-2}. The spectra, at moderately high densities ($\geq 10^{10}$ cm^{-2}) indicate that the initially narrow electron distribution is altered in a time less than or equal to the LO-phonon emission time, as a result of rapid carrier–carrier scattering. At an excitation density of about 10^{10} cm^{-2}, the carrier–carrier scattering rate is faster in narrower quantum wells. By measuring the intensity of the unrelaxed peak, it is possible to determine the relative rates of carrier–carrier scattering and LO-phonon emission. Our results indicate that carrier–carrier scattering becomes as significant as LO-phonon emission at a density of about 1×10^{10} cm^{-2} in the 5 nm quantum wells.

Keywords: A. Quantum wells; D. Electron–electron interactions; D. Optical properties; E. Luminescence

Femtosecond optical spectroscopy has proven to be an excellent tool for the study of fundamental nonequilibrium properties in semiconductors [1–10]. Femtosecond excitation of GaAs can generate an initial highly nonequilibrium electron distribution, which then thermalizes to an equilibrium distribution by carrier–carrier interactions and LO-phonon emission. Thermalization times of 50–300 fs have been deduced from hole burning in transient absorption spectra for excitation below the optical-phonon energy [4–6]. Luminescence up-conversion experiments reveal the rapid redistribution of electrons and holes over a wide energy range, within the first 100 fs after excitation at densities larger than 10^{17} cm^{-3}, demonstrating the dominant role of carrier–carrier scattering at those carrier densities [9]. Carrier–carrier interactions among highly nonequilibrium photoexcited carriers in GaAs have been studied at injected carrier densities from 10^{15} to 10^{17} cm^{-3} in Refs. [3,11,12]. The rate of carrier–carrier scattering within the highly nonequilibrium distribution created by laser excitation is comparable to the LO-phonon emission rate of approximately 1/(150 fs) at carrier densities as low as 1×10^{16} cm^{-3} [13–16].

While there are still questions remaining, it appears safe to say that hot electron relaxation in bulk GaAs is becoming relatively well understood. In reduced dimensionality systems, the effect of quantum confinement on nonequilibrium carriers holds research interest. However, in 2D the situation is quite murky. Less experimental data on carrier–carrier scattering rates are available for 2D than for 3D carriers. The interaction of exciton with free carriers and incoherent excitons in a GaAs single quantum well at 2 K was studied by Honold et al. [17] using time-resolved degenerate four-wave mixing. Kash has studied the energy loss rate of a hot electron to a thermalized electron–hole plasma in $Al_xGa_{1-x}As$/GaAs quantum wells [18]. The experimental situation of nonthermal carrier distributions in 2D has been dominated by four experiments of Knox and coworkers [5,19,20].

In this report, we have made a time-resolved measurement of the distribution at densities below 10^{10} cm^{-2}. We

* Corresponding author. Tel.: +886-4-4517250-3877; fax: +886-4-4510405.

E-mail address: kwsun@fcu.edu.tw (K.W. Sun).

0038-1098/00/$ - see front matter
PII: S0038-1098(00)00189-7

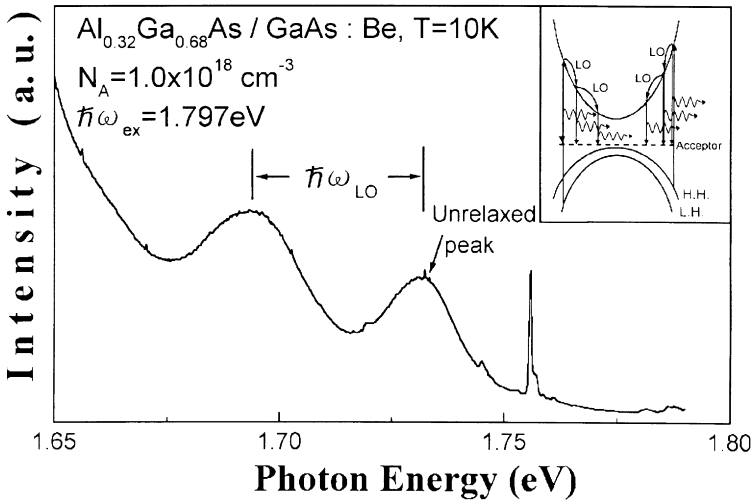

Fig. 1. Time-integrated luminescence of 5 nm quantum wells after CW excitation at 1.797 eV. The schematic of hot electron-neutral acceptor luminescence technique is shown in the inset. The electron distributions are generated both from the heavy- and light-hole bands. The photoexcited electrons have relaxed through successive LO-phonon emission events before recombining with neutral acceptors.

excited the sample with an ultrafast optical pulse and measured the time-integrated hot electron–neutral acceptor (hot(e,A^0)) luminescence spectra as a function of photoexcited carrier densities. We are not only able to inject a moderate density of carriers into the sample we are also able to create highly nonequilibrium distributions of hot carriers with our 120 and 180 fs duration pulses, since LO-phonon emission by the photoexcited carrier is not large during the laser pulses. By measuring the first unrelaxed peak in the hot(e,A^0) luminescence spectra, we are assured of sampling the hot electron distribution within an LO-phonon emission time (~150 fs) [21–26]. Since the luminescence arises from recombination on neutral acceptors and not from band-to-band recombination, we can directly study the early evolution of the hot electron distribution without making assumptions about the shape of the hole distribution.

The MQW samples studied here were 5(3) nm GaAs wells, with $x = 0.32(0.33)$ $Al_xGa_{1-x}As$/GaAsAs barriers of 25 nm thickness. The quantum wells were doped with Be in the central 1 nm of each well to 10^{18} cm^{-3}. The quantum well samples consisted of a stack of 40 wells and were grown on [100] undoped GaAs substrates. For all experiments reported here, the samples were held in a closed-cycle cryostat refrigerator at $T = 10$ K to ensure that virtually all the acceptors are neutral and to reduce the occupancy of LO phonon to insignificant levels. Hot(e,A^0) luminescence spectra are taken with the combination of a triplemate spectrometer and a liquid nitrogen cooled CCD detector. The experiments have employed three excitation sources—an argon ion laser pumped continuous wave (CW) dye laser; a self-mode-locked Ti:sapphire laser; and a mode-locked dye laser. The CW dye laser was operated at energies of 1.797(1.893) eV for the 5(3) nm wells. The self-mode-locked Ti:sapphire laser which generated optical pulses as short as 120 fs was operated at the energy of 1.797 eV with a 80 MHz repetition rate. The mode-locked dye laser is capable of producing 180 fs pulses and is operated at the energy of 1.893 eV with a repetition rate of 100 MHz.

Fig. 1 shows the time-integrated luminescence spectrum of the 5 nm QW sample with the CW dye laser used as the excitation source. The principles of the hot electron–neutral acceptor technique are shown in the inset of Fig. 1. The hot electron luminescence are, typically, many orders of magnitude weaker in intensity than the band-to-band recombination [13]. Therefore, the bandedge signal (at 1.606 eV) is intentionally blocked by a bandpass filter in the spectrometer, in order to observe the hot luminescence spectra. The sharp peak at 1.756 and shoulder at 1.745 eV shown in Fig. 1 are first-order Raman peaks from photon scattering with GaAs- and AlAs-like LO phonons. These peaks will not be analyzed here. In Fig. 1, the “unrelaxed” peak at 1.73 eV is due to the initial unrelaxed hot electrons excited from the lowest heavy hole band recombining with neutral acceptors. In this case, the electron recombines with a hole bound to an impurity, and the luminescence is displaced from the excitation energy by the hole’s excess energy and the binding energy of the acceptor. The peak below this one at 1.695 eV corresponds to electrons that have emitted one LO phonon; however, this coincides with the energy of unrelaxed electrons promoted from the lowest light-hole subbands, so there is ambiguity associated with this second peak. Nevertheless, at low densities, where the carrier–carrier interaction is weak, an initial narrow electron distribution evolves into a series of peaks separated by an LO-phonon energy. This indicates that the 2D photoexcited electrons relaxed through successive LO-phonon emission events before recombining with neutral acceptors.

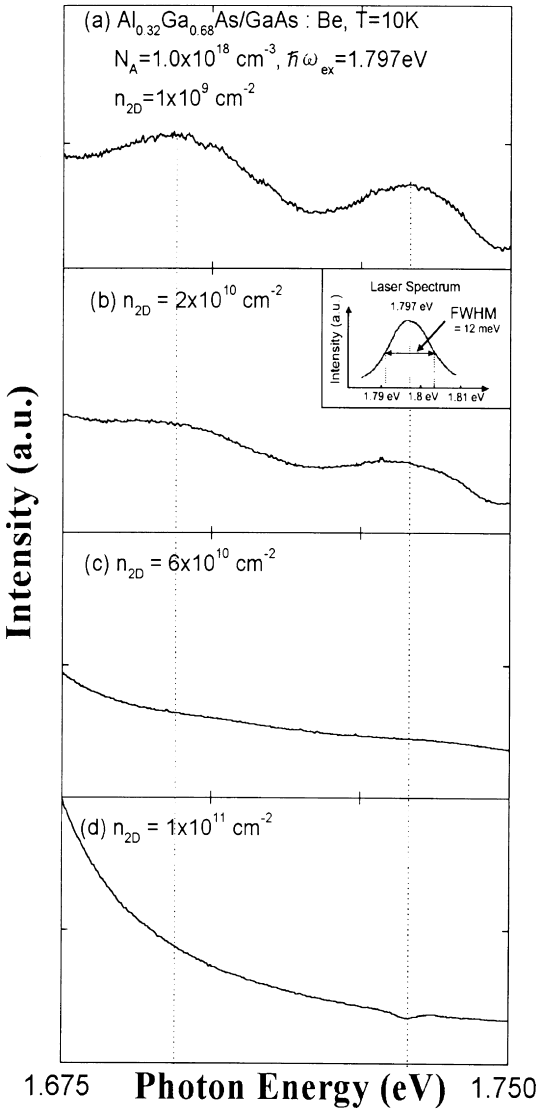

Fig. 2. Time-integrated luminescence of 5 nm quantum wells after femtosecond excitation at 1.797 eV for four injected carrier densities: (a) 1×10^{9} cm^{-2}; (b) 2×10^{10} cm^{-2}; (c) 6×10^{10} cm^{-2}; (d) 1×10^{11} cm^{-2}. The energy spectrum of the 120 fs Ti:sapphire laser pulse is shown in the inset of Fig. 2(b).

In Fig. 2, we show spectra of the 5 nm QW sample obtained with the self-mode-locked Ti:sapphire laser as the excitation source. By changing the laser power, the injected carrier density can be varied with minimal exciton effect. The photoexcited carrier densities are determined from the laser spot size on the sample (through a periscope arrangement behind the entrance slit in the spectrometer) and the absorption coefficient of the QW samples at the photoexcitation wavelength. Our detection system is adjusted to sample only the center half of the laser spot, thus minimizing uncertainties associated with non-uniform injection. Even though the determined carrier densities are only accurate to a factor of two, the density was varied by neutral density filters within an experimental run, therefore, the density dependence can be accurately determined. Injected carrier densities from 1×10^{9} to 2×10^{11} cm^{-2} are obtained by using the mode-locked Ti:sapphire laser as the excitation source, and varying the incident laser power. The corresponding spectra are shown in 2(a)–(d). The unrelaxed peaks begin to decrease at a carrier density of 1×10^{9} cm^{-2}. As the injected carrier density is increased toward 1×10^{11} cm^{-2}, the peaks disappear. The width of the peaks is determined by the electron energy distribution at the point of generation, which is related to the heavy hole subband warping as well as the energy distribution of acceptors, the final state of recombination for the hot luminescence process [13]. We find no change in the linewidth of the peak, and thus measurements of the integrated area under the peak give the same results as measuring the peak height. The probability is small that an electron will be scattered out of this peak before emitting a LO phonon if, during a LO-phonon emission time, scattering transfers little energy among carriers relative to the width of the peak. Thus, at low densities the unrelaxed peak is unaffected by carrier–carrier scattering. However, if scattering processes such as electron–electron scattering and electron–hole scattering are as fast or faster than LO scattering they will yield a broadening of the distribution of electrons sampled by the luminescence measurement. At higher densities, the interactions among carriers are stronger, and at sufficiently high densities carrier–carrier scattering will reduce the height of the unrelaxed peak. The height of the unrelaxed peak thus allowed us to compare the relative importance of carrier–carrier scattering and LO-phonon emission for the scattering of energetic electrons. In Fig. 3, we plot the unrelaxed peak intensity relative to the background (which remains relatively constant) in each spectrum as a function of injected carrier density. We interpret the decrease of the unrelaxed peak as the injected carrier density is increased as evidence that carrier–carrier scattering is becoming important [11,12]. By interpolation, we find that at an injected carrier density of 1×10^{10} cm^{-2}, the intensity drops by a factor of two compared to the CW experiment. Thus, the crossover from scattering dominated by LO-phonon emission to scattering dominated by the carrier–carrier interaction occurs at about this density.

Fig. 4(a) and (b) show the time-integrated hot(e,A^{0}) luminescence spectrum of the 3 nm quantum wells with the CW and mode-locked dye lasers used as the excitation sources. We have used excitation sources operated at appropriate photon energies, in order to give approximately the same amount of excess kinetic energy to the photoexcited carriers as in the 5 nm quantum wells experiments. In Fig 4(a), we can clearly see that the electrons have relaxed through successive LO-phonon emission events before recombining with neutral acceptors as in the 5 nm quantum wells under CW excitation. In Fig 4(b), we show the spectrum obtained

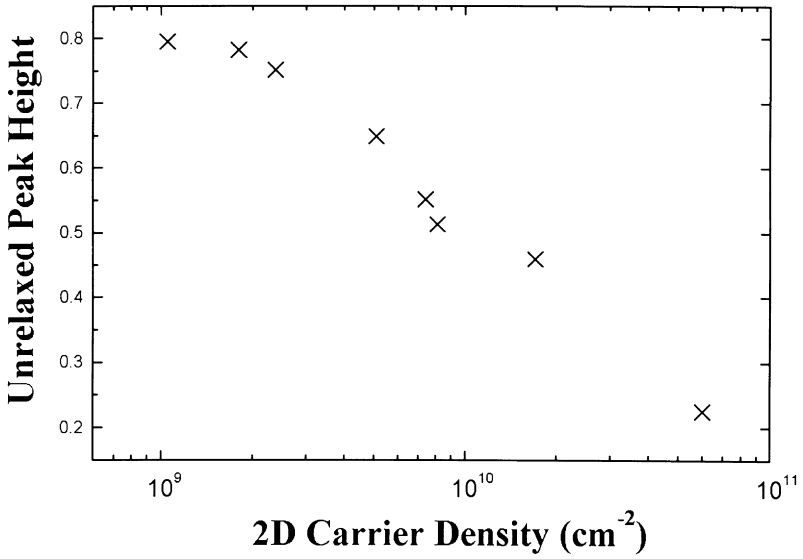

Fig. 3. The unrelaxed peak intensities (relative to the background) in each spectrum taken in the Ti:sapphire laser experiments are plotted as a function of the injected carrier densities.

with the mode-locked dye laser as the excitation source. However, even at an excitation density as low as $10^{10}\,cm^{-2}$, we still observed a featureless spectrum. The absence of any structures with LO-phonon spacing in Fig. 4(b) not only indicates that inelastic carrier–carrier scattering is the dominant mechanism of thermalization but also that the inelastic scattering rates are much faster than in the 5 nm quantum well experiments at about the same density. We attribute this to the stronger quantum confinement and weaker screening in narrower quantum wells.

Only a few calculations of 2D carrier–carrier scattering have as yet explored the dependence of scattering on relevant parameters such as the carrier density. Most of the previous calculations of 2D carrier–carrier scattering have used a static screening model except the Monte Carlo study by El-Sayed et al. [27] and Kane [28] who solved the Boltzmann equation using dynamic screening. Results from our 5 nm QW experiments are in qualitative agreement with Kane's theoretical works in which he has studied the carrier–carrier scattering using an integration of the dynamically screened Boltzmann equation. In his studies, 2D electron–hole pairs are generated in GaAs quantum wells with an average electron energy of 20 meV, and an average hole energy of 12 meV. The initial energy width (FWHM) of the electron peak is 20 meV (corresponding to the energy width of the ultrashort excitation laser pulses). The evolution of the electron distribution is followed for 150 fs. The initial electron peak height dropped by a factor of two as the density was increased to $5\times10^{10}\,cm^{-2}$. In our experiments, by interpolation, we find that at an injected carrier density of $1\times10^{10}\,cm^{-22}$, the unrelaxed peak intensity in Fig. 3 drops by a factor of two compared to the CW experiment. The slight difference between the experimental results and calculations is probably due to the higher electron excess energy for the photoexcited carriers in our experiments. To our knowledge there exist no calculations including dynamic screening, which implies the dependence of carrier–carrier scattering on quantum well width. A thorough calculation by solving a dynamically screened Boltzmann equation with parameters from our experiments is currently under investigation.

We have also found that, in contrast to previous 3D experiments [3,11], the crossover of the two competing processes in 5 nm QW experiments happens at approximately an order of magnitude of lower density (the 3D equivalent density of the crossover density 1×10^{10} is about $1\times10^{15}\,cm^{-3}$). We attribute this to the weaker screening in quantum wells. However, the 2D in-plane mass in the HH_1 subband is different from the 3D heavy hole mass, therefore the heavy holes might play a more important role in 2D experiments than in 3D.

In conclusion, our results from the 5 nm QW experiments show that at an injected density lower than $1\times10^{10}\,cm^{-2}$, the hot electrons lose their energy to the lattice before appreciable carrier–carrier scattering occurs. As the carrier density is increased from 1×10^{9} to $2\times10^{11}\,cm^{-2}$, however, the carrier–carrier scattering begins to compete with carrier-phonon scattering, with a crossover in their relative importance at approximately $1\times10^{10}\,cm^{-2}$. At carrier densities greater than $1\times10^{11}\,cm^{-2}$, carrier–carrier scattering is the dominant scattering process. A qualitative comparison of the carrier–carrier scattering rates in QWs with two different well widths is made by comparing peak height in the hot(e,A^0) luminescence spectra. We have found that carrier–carrier scattering rate is much faster in the

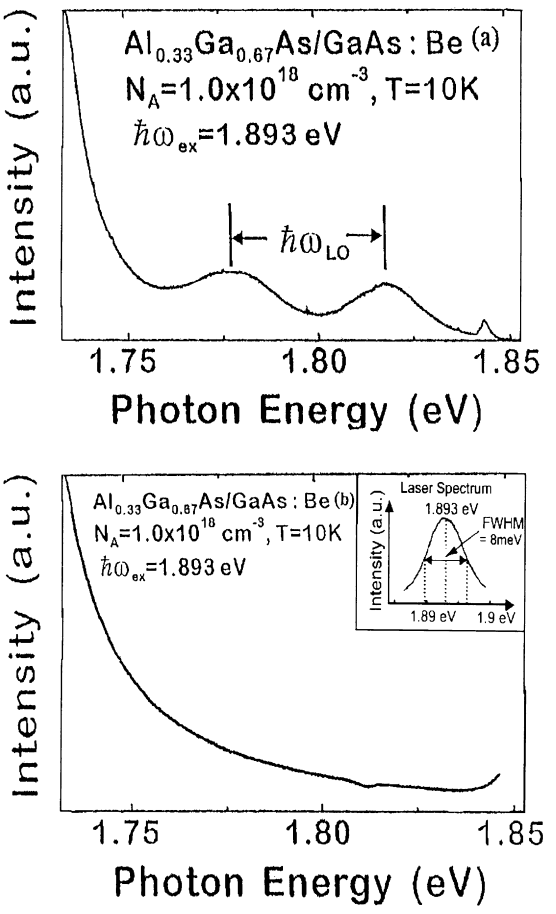

Fig. 4. Time-integrated luminescence of 3 nm quantum wells after: (a) CW, and (b) femtosecond excitation at 1.893 eV. The injected carrier density in spectra (b) is at about 1×10^{10} cm^{-2}. The inset in (b) shows the energy spectrum of the 180 fs dye laser pulse.

narrower wells at an injected carrier density of about 10^{10} cm^{-2}.

Acknowledgements

This work was supported by the National Science Council of the Republic of China under contract Grant no. NSC87-2112-M-035-004 and NSC88-2112-M-035-001.

References

[1] D.W. Snoke, W.W. Rühle, Y.C. Lu, E. Bauser, Phys. Rev. Lett. 68 (1992) 990.
[2] D.W. Snoke, W.W. Rühle, Y.C. Lu, E. Bauser, Phys. Rev. B45 (1992) 10979.
[3] A. Leitenstorfer, C. Fürst, Alaubereau, W. Kaiser, Phys. Rev. Lett. 76 (1996) 1545.
[4] J.L. Oudar, D. Hulin, A. Migus, A. Antonetti, F. Alexandre, Phys. Rev. Lett. 55 (1985) 2074.
[5] W. Knox, C. Hirlimann, D.A.B. Miller, J. Shah, D.S. Chemla, C.V. Shank, Phys. Rev. Lett. 56 (1986) 1191.
[6] J.P. Foing, D. Hulin, M. Joffre, M.K. Jackson, J.L. Oudar, C. Tanguy, M. Combescot, Phys. Rev. Lett. 68 (1992) 110.
[7] C.V. Shank, R.L. Fork, R.F. Leheny, J. Shah, Phys. Rev. Lett. 42 (1979) 112.
[8] J.F. Ryan, R.A. Taylor, A.J. Turberfield, A. Maciel, J.M. Worlock, A.C. Gossard, W. Wiegmann, Phys. Rev. Lett. 53 (1984) 1841.
[9] T. Elsaesser, J. Shah, L. Rota, P. Lugli, Phys. Rev. Lett. 66 (1991) 1757.
[10] J. Shah, B. Deveaud, T.C. Damen, W.T. Tsang, A.C. Gossard, P. Lugli, Phys. Rev. Lett. 59 (1987) 2222.
[11] K.W. Sun, M.G. Kane, S.A. Lyon, Europhys. Lett. 26 (1994) 123.
[12] A. Leitenstorfer, T. Elsaesser, F. Rossi, T. Kuhn, W. Klien, G. Boehm, G. Traenkle, G. Weimann, Phys. Rev. B 53 (1996) 9876.
[13] G. Fasol, W. Hackenberg, H.P. Hughes, K. Ploog, E. Bauser, H. Kano, Phys. Rev. B 41 (1990) 1461.
[14] B.P. Zakharchenya, V.D. Dymnikov, I.Ya. Karlik, I.I. Reshina, J. Phys. Soc. Jpn. 49 (1980) 573.
[15] J.A. Kash, J.M. Hvam, J.C. Tsang, Phys. Rev. Lett. 54 (1985) 2151.
[16] B.P. Zakharchenya, D.N. Mirlin, V.I. Perel, I.I. Reshina, Sov. Phys. Usp. 25 (1982) 143.
[17] A. Honold, L. Schulttheis, J. Kuhl, C.W. Tu, Phys. Rev. B 40 (1989) 6442.
[18] J.A. Kash, Phy. Rev. B 48 (1993) 18336.
[19] W.H. Knox, D.S. Chemla, G. Livescu, J.E. Cunningham, J.E. Henry, Phys. Rev. Lett. 61 (1988) 1290.
[20] W.H. Knox, Solid-State Electron. 32 (1989) 1057.
[21] B.P. Zakharchenya, P.S. Kop'ev, D.N. Mirlin, D.G. Polakov, I.I. Reshina, V.F. Sapega, A.A. Sirenko, Solid State Commun. 69 (1989) 203.
[22] C.V. Shank, R.L. Fork, R. Yen, J. Shah, B.I. Greene, A.C. Gossard, C. Weisbuch, Solid State Commun. 47 (1983) 981.
[23] J. Shah, IEEE J. Quant. Electron. QE-22 (1986) 1728.
[24] S.A. Lyon, Superlattices Microstruct. 3 (1987) 261.
[25] D.N. Mirlin, V.I. Perel, Semicond. Sci. Technol. 7 (1992) 1221.
[26] D. Collings, K.L. Schumacher, F. Raksi, H.P. Hughes, R.T. Philips, Appl. Phys. Lett. 64 (1994) 889.
[27] K. El Sayed, H. Haug, Phys. Status Solidi B 173 (1992) 189.
[28] M.G. Kane, Phys. Rev. B 54 (1996) 16345.